Direct Reactions with Unstable Nuclei

Angela Bonaccorso

INFN, Sez. di Pisa

Italy-Japan 2012

Reaction Theory for Unstable Nuclei

Which is the rôle of Reaction Theory and how simple and/or "complicated vs accurate" does it need to be?

- Understanding the reaction mechanisms.
- Search for the best *observable* to be measured (in view of the reduced intensity of RB).
- Accuracy of methods and numerical implementations.

Plan of the Presentation

Early experiments: halo nuclei

I. Tanihata et al., Phys. Lett. B 160, 380 (1985)

$$\sigma_I = \pi\,[R_I(P) + R_I(T)]^2$$

$$\sigma_R = \pi\left(R_{vol} + R_{surf}\right)^2\left(1 - \frac{B_c}{E_{cm}}\right)$$

Kox et al. (1987)

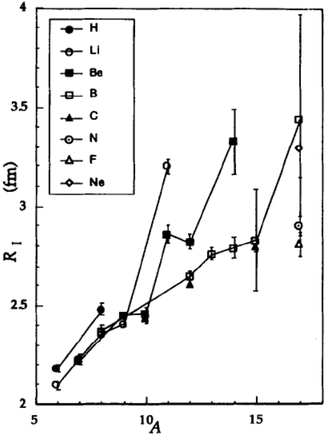

Fig. 2.1 Interaction cross sections of light nuclei determined by 800A MeV reactions.

Early eikonal model

I. Tanihata, Prog. Part. Nucl. Phys. 35, 505 (1995)

These equations provide a simple way to compare the reaction cross sections at different energies. However, since they are purely empirical formula, one should be careful when applying them to an exotic nucleus because of a possible difference in the surface diffuseness as well as any proton-neutron density difference. When one measures σ_R using a β-unstable nucleus, only r_0 is expected to change.

$$\sigma_R = \int_0^\infty d\mathbf{b}(1 - |S(\mathbf{b})|^2) = \sigma_{ct} + \sigma_{nt}$$

decoupling of core and halo

$$\rho_p = \rho_c + \rho_n \quad (1)$$

$$|S(\mathbf{b})|^2 = e^{-[\sigma_{nn} \int ds \rho_p(|b-s|)\rho_t(s)]} = e^{-[\sigma_{nn} \int ds \rho_c \rho_t]} e^{-[\sigma_{nn} \int ds \rho_n \rho_t]}$$

$$\sigma_{nt} = \int_0^\infty d\mathbf{b} |S_{ct}(\mathbf{b})|^2 P_{b_{up}}(\mathbf{b})$$

(!)⊗

Early theory: halo nuclei

P. G. Hansen and B. Jonson, Europhys. Lett., 4, 409 (1987).
see also B. Jonson, PR389 (2004).

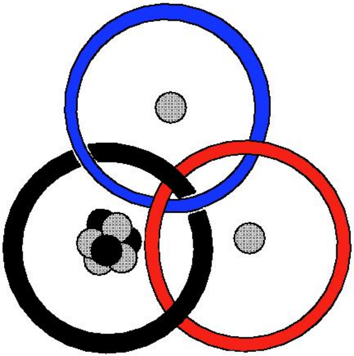

- Large spatial extension
- One- or two- neutron halo nuclei
- Two neutron halo (Borromean Systems): ^{6}He, ^{11}Li, ^{14}Be
- Three-body model
- Importance of the n-core interaction
  n-^{9}Li, n-^{12}Be (+)

Reaction theory: K. Yabana, Y. Ogawa,Y. Suzuki (1992); H. Sagawa, N.Takigawa (1994), H. Esbensen and GF. Bertsch; C. Bertulani and W.Bauer; M. Hussein and KW. MacVoy; Barranco, Vigezzi & Broglia, G. Hansen(1996). Structure theory: Zhukov and Thompson, Surrey group, Nordic collaboration

First attempt to disentangle breakup reaction mechanisms

CALCULATION: J. Margueron, A.B, D. M. Brink *Coulomb-nuclear coupling and interference effects in the breakup of halo nuclei*

J. Margueron et al. / Nuclear Physics A 703 (2002) 105–129   119

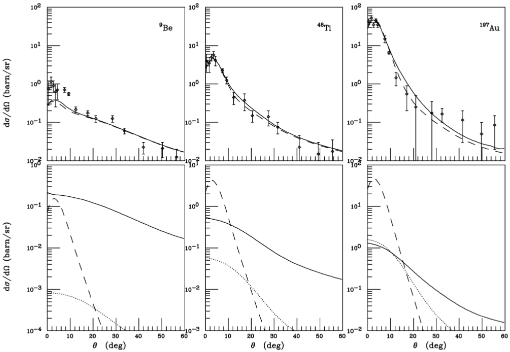

Fig. 5. Neutron angular distributions following breakup of ^{11}Be at 41 A.MeV for several targets (^{9}Be, ^{48}Ti, ^{197}Au). In the bottom figures the nuclear distribution is represented by the solid line, Coulomb by the long dashed line, and the Coulomb-nuclear term by the dotted line. In the top figures the coherent sum of the nuclear, Coulomb and Coulomb-nuclear terms by the solid line, the nuclear plus the perturbative Coulomb incoherent sum by the dashed line. Experimental points are from Anne [25].

DATA: R. Anne et al., PLB250, 19 (1990), PLB304 55 (1993), NPA 575 125 (1994).

Transfer to the continuum reaction (inclusive)

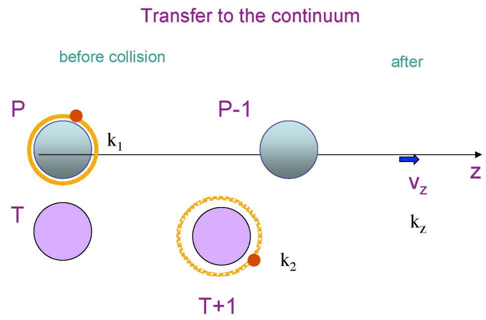

$k_2 - k_1 = k_z$
$\varepsilon_f - \varepsilon_i = mv^2/2$

++

Transfer to the continuum (Knockout)

F. Flavigny, A. Obertelli, AB et al., PRL108 252501 (2012). **

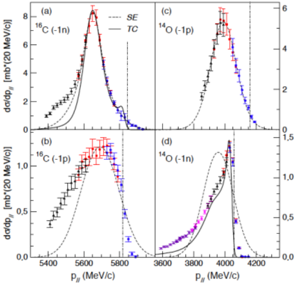

J.Enders et al. PHYSICAL REVIEW C 65 034318

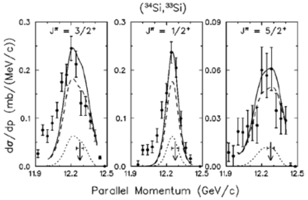

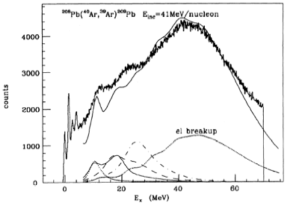

AB et al., PRC49(1994)

Transfer to continuum (Resonances)

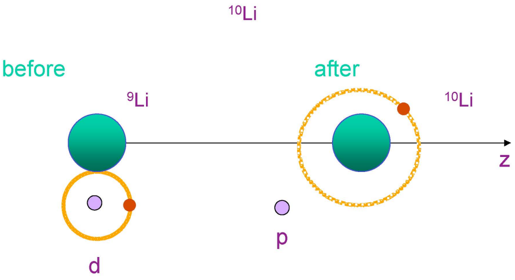

(+)

^{9}Li (d,p) REX-ISOLDE, H.B. Jeppesen, PLB642, 449 (2006),
G.Blanchon, AB, N. Vinh Mau, NPA739, 259 (2004).

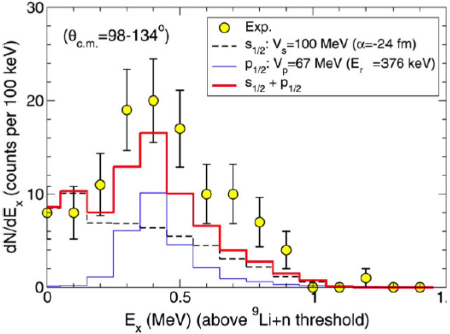

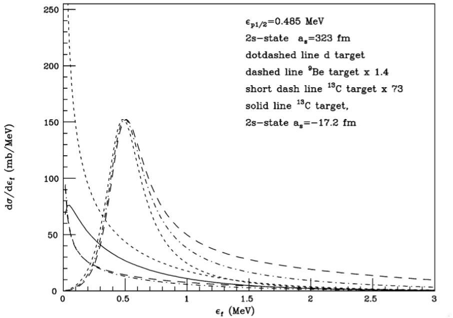

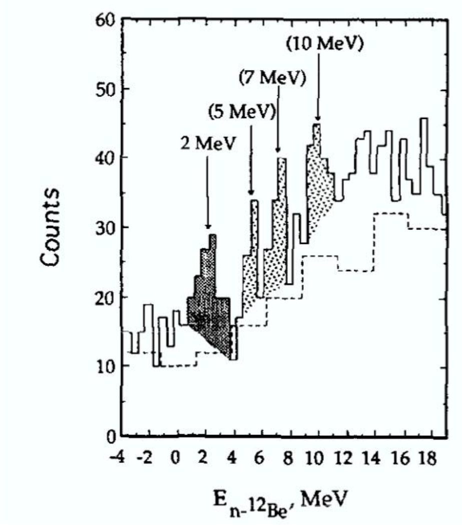

Figure: ^{12}Be (d,p) RIKEN (Korsheninnikov) (1995)

Fragmentation reaction (coincidence)

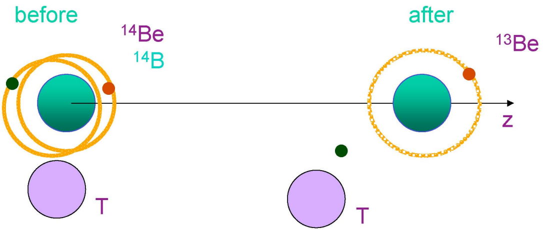

$* * *$ $(+)$

Fragmentation (^{10}Li best example)

GSI, H. Simon et al. NPA791 (2007) 267; G. Blanchon et al. NPA791 (2007) 303

Table 3
Scattering length of the 2s continuum state, energies and widths of the p- and d-resonances in ^{10}Li and corresponding strength parameters for the δV potential

	ε_{res} (MeV)	Γ_j (MeV)	a_s (fm^{-1})	α (MeV)
$2s_{1/2}$			-17.2	-10.0
$1p_{1/2}$	0.63	0.35		3.3
$1d_{5/2}$	1.55	0.18		-9.8

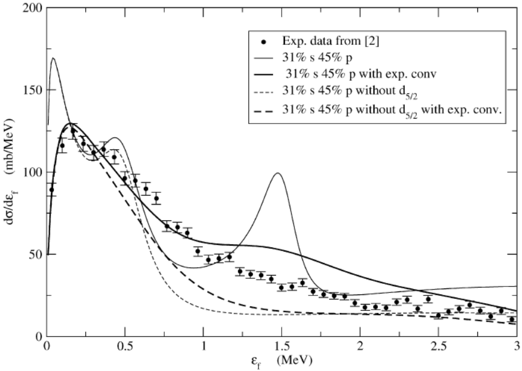

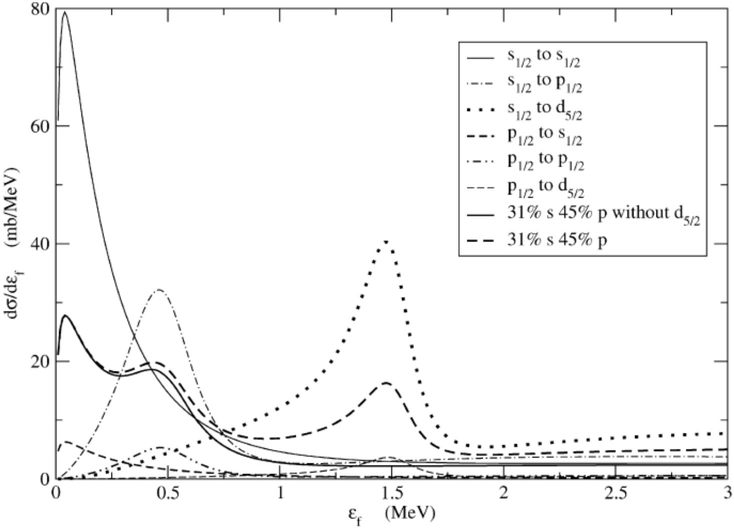

80
60
40
20
0
dσ/dε_f (mb/MeV)
0
0.5
1
1.5
2
2.5
3
ε_f (MeV)
s_1/2 to s_1/2
s_1/2 to p_1/2
s_1/2 to d_5/2
p_1/2 to s_1/2
p_1/2 to p_1/2
p_1/2 to d_5/2
31% s 45% p without d_5/2
31% s 45% p

Coulomb breakup (inclusive or coincidence)

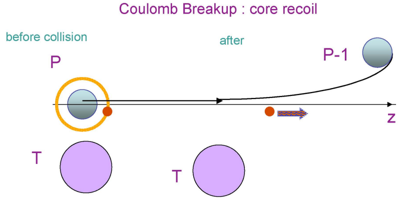

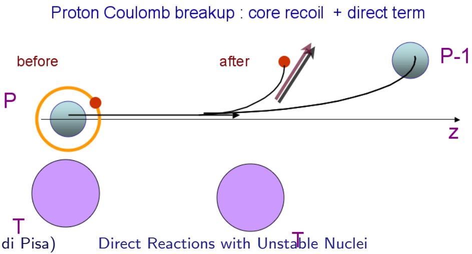

Sketch of coordinates

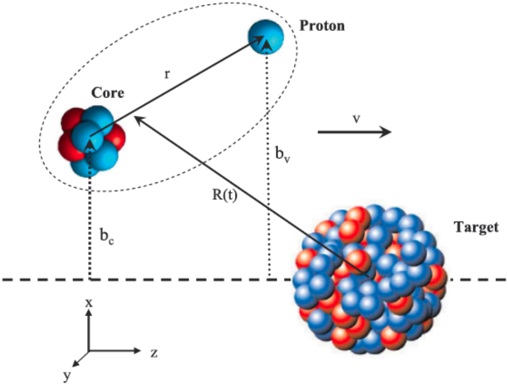

A consistent formalism for various breakup reactions

The core-target movement is treated in a semiclassic way, but neutron-target and/or neutron-core in a full QM treatment.

AB and DM Brink, PRC38, 1776 (1988), PRC43, 299 (1991), PRC44, 1559 (1991).

$$\frac{d\sigma}{d\varepsilon_f} = C^2 S \int_0^\infty d\mathbf{b_c} \frac{dP_{-n}(b_c)}{d\varepsilon_f} P_{ct}(b_c),$$

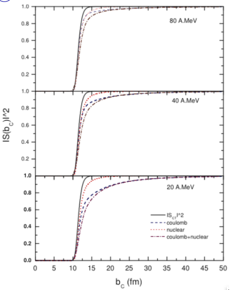

Use of the simple parametrization
$P_{ct}(b_c) = |S_{ct}|^2 = e^{(-\ln 2 exp[(R_s - b_c)/a])}$,

$$R_s \approx 1.4(A_p^{1/3} + A_t^{1/3}) fm$$

'strong absorption radius'.

Two aspects are important:

Shape of the spectra, Absolute cross sections

Transfer to the continuum

First order time dependent perturbation theory amplitude:

$$A_{fi} = \frac{1}{i\hbar}\int_{-\infty}^{\infty} dt < \phi_f(\mathbf{r})|V(\mathbf{r})|\phi_i(\mathbf{r}-\mathbf{R}(t)) > e^{-i(\omega t - mvz/\hbar)} \qquad (2)$$

$$\omega = \varepsilon_i - \varepsilon_f + \frac{1}{2}mv^2$$

$$\frac{dP_{-n}(b_c)}{d\varepsilon_f} = \frac{1}{8\pi^3}\frac{m}{\hbar^2 k_f}\frac{1}{2l_i+1}\Sigma_{m_i}|A_{fi}|^2$$

$$\approx \frac{4\pi}{2k_f^2}\Sigma_{j_f}(2j_f+1)(|1-\bar{S}_{j_f}|^2 + 1 - |\bar{S}_{j_f}|^2)\mathcal{F},$$

see also Trojan horse

$$\mathcal{F} = (1 + F_{l_f,l_i,j_f,j_i})B_{l_f,l_i}$$

$$B_{l_f,l_i} = \frac{1}{4\pi}\left[\frac{k_f}{mv^2}\right]|C_i|^2\frac{e^{-2\eta b_c}}{2\eta b_c}M_{l_f l_i}$$

Kinematics

From Eq.2 by the change of variables $dtdxdydz \to dxdydzdz'$
$e^{-i(\omega t - mvz/\hbar)} \to e^{-ik_1 z'} e^{ik_2 z}$ neutron energies to neutron parallel momenta with respect to core

$$k_1 = \frac{\varepsilon_f - \varepsilon_i - \frac{1}{2}mv^2}{\hbar v};$$

to target

$$k_2 = \frac{\varepsilon_f - \varepsilon_i + \frac{1}{2}mv^2}{\hbar v};$$

to core parallel momentum

$$P_{//} = \sqrt{(T_p + \varepsilon_i - \varepsilon_f)^2 + 2M_r(T_p + \varepsilon_i - \varepsilon_f)}, \quad (3)$$

breakup threshold at $\varepsilon_f = 0$
$++**$

Example of kinematical effects PRC60(1999) 054604,PRC44(1991) 1559

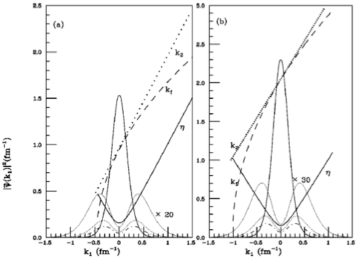

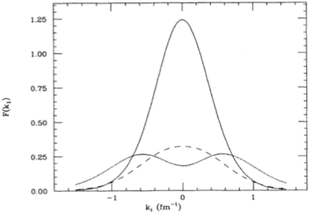

FIG. 11. Initial-state momentum distributions in ^{20}Ne according to Eq. (2.3a). The solid curve is for the $2s_{1/2}$ state, the dashed curve is the for $1p_{1/2}$, while the dotted curve is for the $1d_{5/2}$ state.

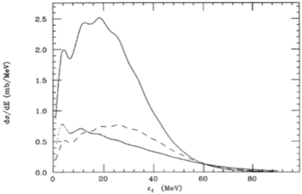

FIG. 7. Calculated total spectrum of the reaction ^{208}Pb(^{20}Ne,^{19}Ne)^{209}Pb at $E_{\rm inc}=40$ MeV/nucleon. The solid curve is for the $2s_{1/2}$ initial state, the dashed curve is for the $1p_{1/2}$ initial state, while the dotted curve is for the $1d_{5/2}$ initial state.

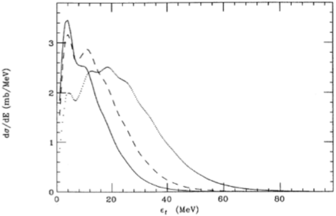

FIG. 8. Calculated total spectrum of the reaction ^{208}Pb(^{20}Ne,^{19}Ne)^{209}Pb for the $2s_{1/2}$ initial state. The solid curve is at $E_{\rm inc}=25$ MeV/nucleon, the dashed curve is at $E_{\rm inc}=30$ MeV/nucleon, and the dotted curve is at $E_{\rm inc}=40$ MeV/nucleon.

(+)

Example of kinematical effects AB and GF Bertsch, PRC63(2001) 044604; F. Flavigny et al., PRL108 252501 (2012).

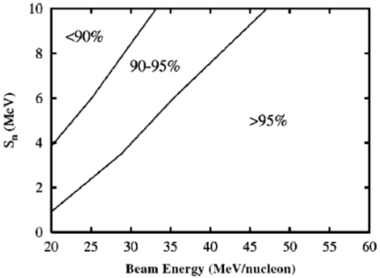

FIG. 1. Ratio of phase space integrals with and without momentum cutoffs, for a d-wave neutron wave function. The effect of the cutoff is to include less than 90%, between 90% and 95%, and more than 95% of the initial momentum distribution as marked on the figure.

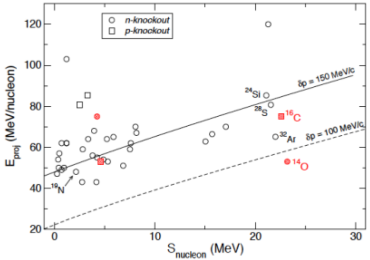

FIG. 3: (Color online) Nucleon-removal experiments from the literature [7, 22, 34] plotted as a function of the energy per nucleon of the projectile and the separation energy of the removed nucleon. The lines correspond to cutoffs appearing at $\delta p = 100$ and 150 MeV/c with respect to the center of the SE distribution. Data from the present experiment are in red.

Eikonal limit

Small neutron scattering angles

$$M_{l_f l_i} \approx P_{l_i}(X_i) P_{l_f}(X_f); \qquad P_{l_f}(X_f) \to J_0(2\eta \mathbf{b_v})$$

large n-t angular momenta

$$\frac{4\pi}{2k_f^2} \Sigma_{j_f}(2j_f + 1) \to \int_0^\infty d\mathbf{b_v}$$

both conditions might not be well satisfied for stripping of deeply bound nucleons unless the core-target scattering is very peripheral. Verify core angular distributions.

$$P_{-n}(\mathbf{b_c}) = \int_0^\infty d\mathbf{b_v}(|1 - \bar{S}(b_v)|^2 + 1 - |\bar{S}(b_v)|^2)|\tilde{\phi}_i(|\mathbf{b_v} - \mathbf{b_c}|, k_1)|^2$$

Notice $k_1 \to -\infty$ not strictly necessary.

Coulomb breakup

Bertulani&Baur, Typel, Surrey group,Bertsch&Esbensen, Baye &Co.

- Contradictory experimental results on the existence of a proton halo.
- Candidates ^{8}B and ^{17}F, both weakly bound, strong astrophysical interest.
- Hypothesis: proton behaves like a neutron with a larger (effective) separation energy.

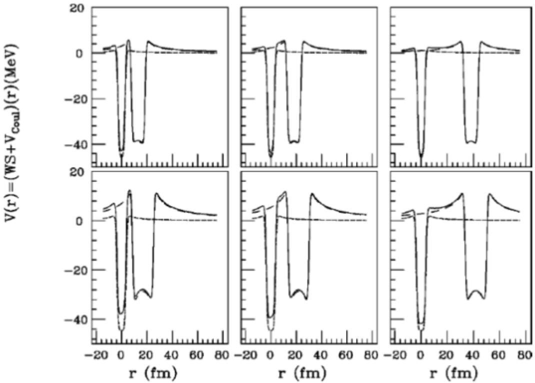

TABLE I. Barrier radii, initial binding energies, and effective energy parameters for a ^{208}Pb target.

	^{8}B	J^{π}	^{17}F	J^{π}
R_i (fm)	6.0		6.5	
ε_i (MeV)	−0.14	$1p_{3/2}$	−0.6	$1d_{5/2}$
ε_i^* (MeV)	−0.57	$1p_{1/2}$	−0.1	$2s_{1/2}$
$-\Delta$ (MeV)	−0.4		−1.2	
$\bar{\varepsilon}_i$ (MeV)	−0.54	$1p_{3/2}$	−1.8	$1d_{5/2}$
$\bar{\varepsilon}_i^*$ (MeV)	−0.97	$1p_{1/2}$	−1.3	$2s_{1/2}$

FIG. 2. Nuclear-Coulomb potentials for ^{8}B + ^{58}Ni (top) and ^{17}F + ^{208}Pb (bottom) at distances between the centers equal to $d=1.4(A_p^{1/3}+A_T^{1/3})$ fm $+s$, with $s=5$, 15, and 30 fm. Short and long dashed lines are the projectile and target potentials, respectively. Full line is the projectile-target combined potential.

AB, DM Brink, C. Bertulani, PRC69 024615(2004).

A. García-Camacho et al., PRC76, 014607 (2007)

Ravinder Kumar and AB, PRC84, 014613 (2011)

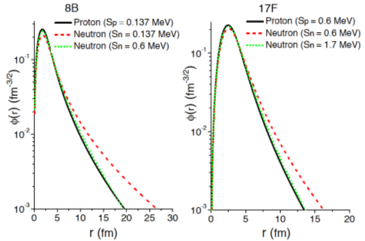

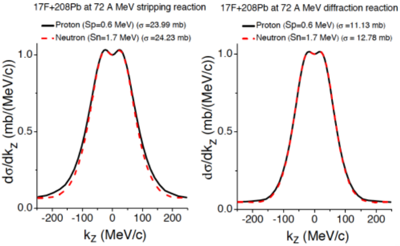

OK for nuclear breakup.

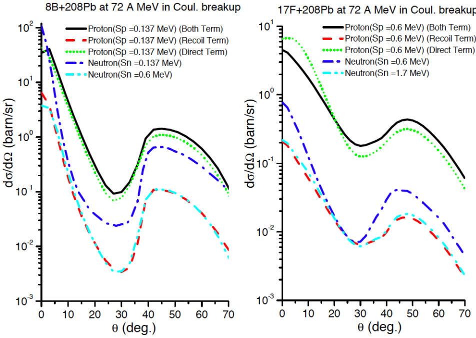

- More complicated for Coulomb breakup because of the direct p-t Coulomb term.
- Proton angular distributions are the "clean" observable.

PHYSICAL REVIEW C 86, 034601 (2012)

Y. KUCUK AND A. M. MORO

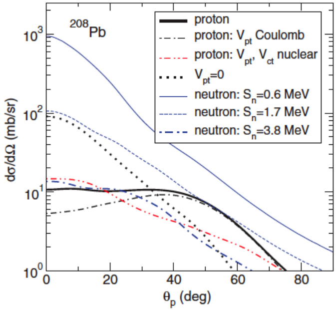

FIG. 8. (Color online) Proton angular distribution following the breakup of ^{17}F on ^{208}Pb at 170 MeV. See text for details.

The interplay of nuclear and Coulomb effects in proton breakup from exotic nuclei

Ravinder Kumar[a,b] and Angela Bonaccorso[a]

TABLE II: $\sigma_{b_{up}}$(mb) for nuclear and Coulomb mechanisms as indicated, for ^{8}B, 1p$_{3/2}$ initial state, and ^{17}F, 1d$_{5/2}$ initial state, on ^{12}C and ^{208}Pb targets at E$_{inc}$=40, 60, 80MeV.

Target	^{12}C						^{208}Pb					
E$_{inc}$(A.MeV)	40		60		80		40		60		80	
Projectile	^{8}B	^{17}F	^{8}B	^{17}F	^{8}B	^{17}F	^{8}B	^{17}F	^{8}B	^{17}F	^{8}B	^{17}F
Stripping	51.62	18.06	41.17	13.49	34.79	10.93	105.94	29.97	88.59	23.09	78.16	19.29
Diffraction	31.72	8.19	23.16	5.42	18.86	4.15	70.42	14.08	58.84	10.99	52.39	9.36
Coulomb recoil	0.10	0.007	0.05	0.004	0.03	0.002	534.18	65.98	262.23	31.74	159.09	19.14
Coulomb direct	2.09	0.58	1.01	0.28	0.61	0.17	4562.66	1209.35	2578.76	624.61	1741.04	394.54
Total Coulomb	2.51	0.67	1.21	0.32	0.73	0.19	4129.47	1542.39	2796.84	874.40	1925.34	611.52
Coulomb and Diffraction	60.29	22.79	39.74	13.18	30.89	9.42	4228.56	1608.39	2740.82	956.64	1928.03	691.09

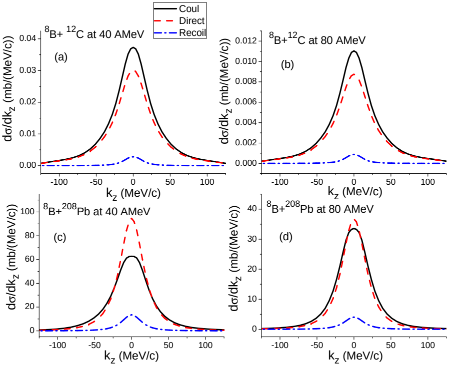
Coul
Direct
Recoil
^{8}B+ ^{12}C at 40 AMeV
(a)
^{8}B+^{12}C at 80 AMeV
(b)
^{8}B+^{208}Pb at 40 AMeV
(c)
^{8}B+^{208}Pb at 80 AMeV
(d)
dσ/dk$_z$ (mb/(MeV/c))
k$_z$ (MeV/c)

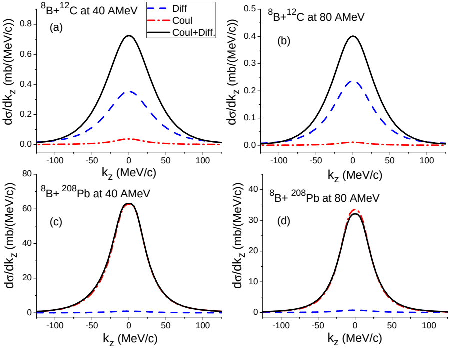
Diff
Coul
Coul+Diff.
^{8}B+^{12}C at 40 AMeV
(a)
^{8}B+^{12}C at 80 AMeV
(b)
^{8}B+ ^{208}Pb at 40 AMeV
(c)
^{8}B+ ^{208}Pb at 80 AMeV
(d)
dσ/dk$_z$ (mb/(MeV/c))
k$_z$ (MeV/c)

^{14}Be structure

The ground state of ^{14}Be has spin $J^{\pi} = 0^{+}$. In a simple model assuming two neutrons added to a ^{12}Be core in its ground state the wave function is:

$$|^{14}Be >= [b_1(2s_{1/2})^2 + b_2(1p_{1/2})^2 + b_3(1d_{5/2})^2] \otimes |^{12}Be, 0^{+} >$$

Then the bound neutron can be in a 2s, $1p_{1/2}$ or $1d_{5/2}$ state. However, the situation is much more complicated and in particular the calculations of Tarutina, Thompson and Tostevin show that there is a large component $(2s_{1/2}, 1d_{5/2}) \otimes |^{12}Be, 2^{+} >$ with the core in its low energy 2^{+} state which can modify the neutron distribution.

^{13}Be experimentally

It is experimentally proved that

- ^{13}Be is not bound
- $5/2^{+}$ resonance at 2MeV
- $S_{2n}(^{14}\mathrm{Be}) = 1.34 \pm 0.11$MeV

Fragmentation of a 2n-halo nucleus * * *

Inelastic-like excitations can be described by the first order time dependent perturbation theory amplitude ⊗:

$$A_{fi} = \frac{1}{i\hbar} \int_{-\infty}^{\infty} dt \langle \psi_f(t) | V_2(\mathbf{r} - R(t)) | \psi_i(t) \rangle$$

This method has the advantage that different potentials can be used for the determination of ψ_i and ψ_f.
Which components of the initial wave function show up in the continuum??

Determination of the bound and unbound (via optical model n-core S-matrix) states.

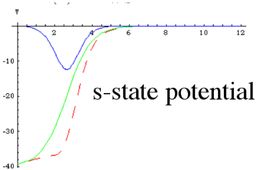

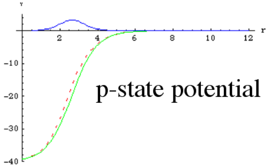

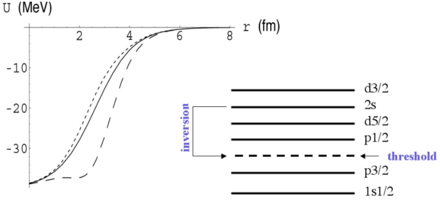

$$U(r) = V_{WS} + \delta V$$

$$\delta V(r) = 16\alpha \frac{e^{2(r-R)/a}}{(1+e^{(r-R)/a})^4}$$

V_{WS} = Woods-Saxon + Spin orbit
δV = Correction to the potential originated from p.v. coupling (*N. Vinh Mau and J. C. Pacheco, NPA607 (1996) 163*)

Fragmentation: (^{13}Be puzzle)

(a)

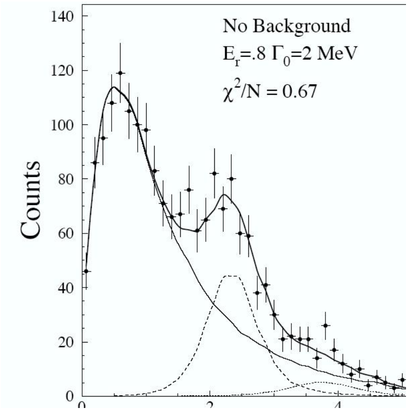

Figure: (a) LPC & GANIL, Lecouey, Orr et al. 2002.

(b)

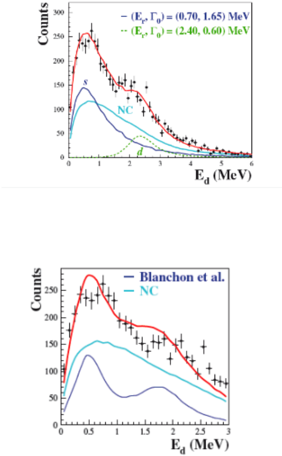

Figure: (b) LPC & GANIL, G. Randisi, N.Orr et al. 2012, DREB12's talk and private comm.

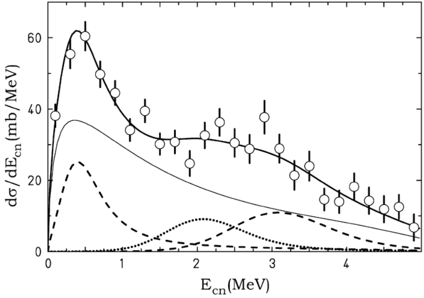

Figure: (a) GSI, H. Simon et al. NPA791 (2007) 267.

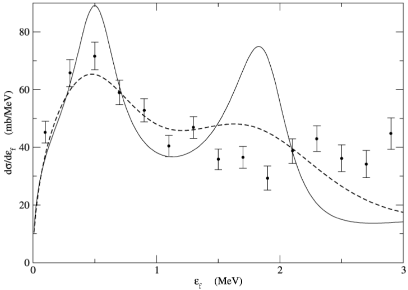

Figure: (b) G.Blanchon et al. NPA784 (2007) 49.

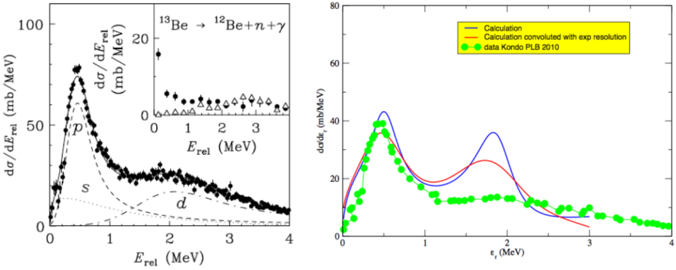

Figure: (b) RIKEN, Y. Kondo et al. PLB690 (2010) 245; G. Blanchon, private communication.

Theoretical models (structure)

- Generator coordinate model (Descouvemont)
- Lagrangian mesh calculation (Baye)
- Fadeev calculation (Zhukov and Thompson)
- Macroscopic model with deformation (Tarutina, Thompson, Tostevin)
- RPA particle-particle (Pacheco and Vinh Mau)
- Antisymmetrized molecular dynamics (Y. Kanada-En'Yo)

^{12}Be and ^{14}Be in pp-RPA: inversion (B), non inversion (A)

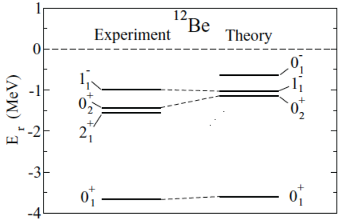

FIG. 1. Low-lying spectra of ^{12}Be obtained with pp-RPA compared to experiment.

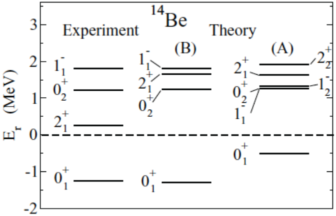

FIG. 3. Low-lying spectra of ^{14}Be obtained with pp-RPA without (A) and with (B) inversion in ^{13}Be compared to experiment.

	$S_{2n}(^{12}\mathrm{Be})$	$S_{2n}(^{14}\mathrm{Be})$	$\langle \mathbf{r}^2\rangle^{1/2}_{A+2}$	$\langle \rho^2\rangle^{1/2}$	$\langle \lambda^2\rangle^{1/2}$
A	2.91	0.51	3.45	8.45	5.45
B	3.71	1.29	2.91	4.56	4.02
Experimental	3.673 ± 0.015	1.26 ± 0.01	3.10 ± 0.15	5.4 ± 1.0	4.2 ± 1.7

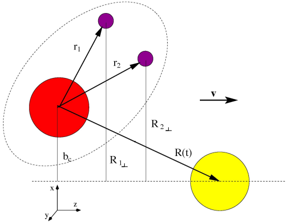

Strength of every transition

Gives information about the 'mother' nuclei

Dependence on the scattering length of the final s-state

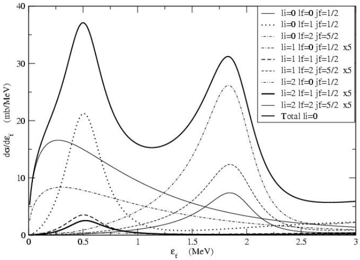

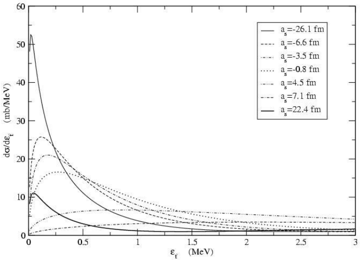

Past-Present-Future

My whish-list:

- Knockout: kinematical complete experiments with reconstruction of target final state.
- Projectile-fragmentation...perhaps the most difficult experiments to make...and interpret?
- More proton breakup experiments since we now understand better the dynamics.
- The past has been characterized by studies at high incident energy and for weakly bound projectiles. In the future more and more strongly bound nuclei will be studied at lower energies at ISOL-type facilities.

EURISOL NET

Some of my co-authors, in historical order:

D. M. Brink
N. Vinh Mau
F. Carstoiu
J. Margueron
G. Blanchon
G. F. Bertsch
C. Bertulani
Awad Ibraheem
M. Thoenessen, A. Spyrou and the MONA collaboration
A. García-Camacho
Ravinder Kumar
L. Trache, A.Banu
C. Rea
the MAGNEX group (LNS-CT)
L. Sobotka, R. Shane
F. Flavigny, A. Obertelli